

Cite this: *RSC Adv.*, 2015, 5, 6340Received 13th September 2014  
Accepted 11th December 2014

DOI: 10.1039/c4ra10346g

www.rsc.org/advances

## Characterization of a thin, uniform coating on P2-type $\text{Na}_{2/3}\text{Fe}_{1/2}\text{Mn}_{1/2}\text{O}_2$ cathode material for sodium-ion batteries†

Kwangjin Park,\* Dongwook Han, JeongKuk Shon, Seok Gwang Doo and Seoksoo Lee

A thin, uniform carbon coating on  $\text{Na}_{2/3}\text{Fe}_{1/2}\text{Mn}_{1/2}\text{O}_2$  (NFMO) using 2,3-dihydroxynaphthalene (DN) was prepared. Pristine and DN-coated samples were characterized by X-ray diffraction (XRD), scanning electron microscopy (SEM), and transmission electron microscopy (TEM). An amorphous nanolayer coating of carbon is obtained on the surface of the layered pristine material. The 0.2 wt% DN-coated NFMO exhibits excellent electrochemical performance. An initial discharge capacity of  $178 \text{ mA h g}^{-1}$  was obtained at a C-rate of 0.1 C; this capacity is 20% higher than bare NFMO. Capacity retention (77.8% at the 50th cycle) is also maintained comparable to bare NFMO (77.7% at the 50th cycle). The thin and uniform carbon layer leads to improvement of charging and discharging kinetics and protects against direct contact between cathode and electrolyte.

### Introduction

Recently, Interest in lithium-ion batteries, which have a high energy density, has been rapidly increasing because of their potential use in applications ranging from mobile products to high-energy-capacity devices such as electric vehicles (EV) and energy-storage systems (ESS).<sup>1–4</sup> However, because of the limited amount of Li reserves on Earth (0.006 wt% abundance on Earth), their cost is relatively high. Thus, alternative battery materials are actively sought. Sodium ion secondary batteries (SIBs) have attracted attention due to abundant resources and low costs.<sup>1–4</sup> However, it is difficult to find an electrode into which sodium can be readily inserted and de-inserted, owing to the large standard electrode potential. Over the past decades, considerable effort has been devoted to the development of layered transition metal oxides such as  $\text{Na}_x\text{MO}_2$  ( $\text{M} = \text{Co}, \text{Ni}, \text{Mn}, \text{Cr}, \text{Fe}$ ) as active cathode materials.<sup>5–13</sup> Recently, P2-

type  $\text{Na}_{2/3}\text{Fe}_{1/2}\text{Mn}_{1/2}\text{O}_2$  (NFMO) cathode has been reported to show the best capacity ( $190 \text{ mA h g}^{-1}$ ).<sup>1</sup> However, this fascinating layered oxide cathode still has several major drawbacks that need to be overcome for commercialization, such as higher irreversible initial-capacity loss and low rate-capability.<sup>7</sup> In general, it is known that surface modification of cathode materials, *e.g.*, by applying a surface coating, is effective to improve electrochemical performance. Electrochemically inert oxide materials, such as  $\text{Al}_2\text{O}_3$  and  $\text{ZrO}_2$ , have been used for the coating.<sup>8–10</sup> Lithium-ion battery cathodes coated with these oxides have improved cycle performance as a result of the blocking of direct contact between the electrolyte and cathode.<sup>8–10</sup> Carbon coating is also an effective surface-modification approach to increase electronic conductivity and improve electrochemical performance.<sup>11–13</sup> Research on Li-ion batteries has indicated that carbon coating is a promising method to improve electrochemical performance.<sup>11–14</sup> A similar effect for Na-ion batteries was confirmed using Na super ionic conductor (NASICON) by Y. Lu *et al.* and Z. Jian *et al.*<sup>15,16</sup> However, the capacity was still not large when NASICON was used even though the carbon coating and the coated surface of NASICON were not uniform. Moreover, coating of uniform and thin carbon layers on the surface of transition metal oxides with a layered crystal structure has not been possible. This has been mainly due to the extensive structural degradation of the layered oxides as a result of the reduction of the core transition metal ions, resulting from the oxidation of carbon sources, at high synthetic temperatures. 2,3-Dihydroxynaphthalene (DN) is a candidate material for carbon coating on layered-oxide SIB cathode materials with minimal damage to the pristine material. T. Kwon *et al.* and H. Nishihara *et al.* reported the formation of a uniform carbon coating on the surface of porous silica.<sup>17,18</sup> Moreover, using DN, an extremely thin and uniform layer can be realized on the surface, leading to increased electrical conductivity of the cathode and prevention of direct contact between the electrolyte and cathode. Furthermore, there is no structural or morphological change in the bare material during the coating process.

Samsung Advanced Institute of Technology (SAIT), Samsung Electronics, Mt. 14-1, Nongseo-dong, Giheung-gu, Yongin-si, Gyeonggi-do 446-712, Republic of Korea. E-mail: ydmj79.park@samsung.com; Fax: +82-31-8061-1319; Tel: +82-31-8061-1250

† Electronic supplementary information (ESI) available. See DOI: 10.1039/c4ra10346g

In this paper, the electrochemical performance of uniformly carbon-coated NFMO is reported. A very thin and uniform carbon layer was prepared by using DN. A 25% increase in initial capacity and capacity retention of 77.8% after the 50th cycle were obtained utilizing 0.2 wt% DN-coated NFMO. In addition, the influence of the coating layer on the morphology and electrochemical performance of the carbon-coated NFMO (NFMO/C) cathode were investigated.

## Experiment

NFMO was prepared by a solid-state reaction from stoichiometric amounts of  $\text{Na}_2\text{CO}_3$ ,  $\text{Fe}_2\text{O}_3$ , and  $\text{Mn}_2\text{O}_3$  with molar ratios of  $2/3 : 1/2 : 1/2$ . The sample mixture was heated for 12 h at  $900^\circ\text{C}$  in air. To achieve complete carbon coating on the active material, the proper amount of DN according to the desired weight percent was dissolved in 5 ml of ethanol and the solution was poured into dried NFMO. The mixture was stirred at room temperature and oven-dried at  $80^\circ\text{C}$  to evaporate the ethanol. The resulting solid mixture of DN and NFMO was heat-treated at  $550^\circ\text{C}$  for 3 h under  $\text{N}_2$  flow.

The sample structures were determined by X-ray diffraction (XRD), using  $\text{Cu K}\alpha$  radiation, a scan speed of  $0.02^\circ$  per minute between  $10^\circ$  and  $65^\circ$  and an applied potential of 40 kV and current of 40 mA. X-ray photoelectron spectroscopy (XPS) analyses were performed with a  $\Phi$  Physical Electronics spectrometer (QUANTUM 2000 scanning ESCA microprobe) using focused monochromatized  $\text{Al K}\alpha$  radiation (1486.6 eV). To avoid external contamination, all samples were transferred under an inert gas from the glove box to the spectrometer using a transfer chamber. Morphology changes of the NFMO were determined using a scanning electron microscope (SEM), (Hitachi S-4700N). Transmission electron microscope (TEM) images were obtained with a JEOL JEM-2010, at an acceleration voltage of 200 V, to verify the morphology of the coating layer of NFMO/C particles. The electrical conductivity of the powder sample was measured with the 4-probe method that we have previously developed.<sup>6</sup>

Composite positive electrodes comprising 60 wt% active materials, 20 wt% Denka black, and 20 wt% polyvinylidene difluoride (PVDF) were pasted onto an aluminum foil as a current collector. The electrodes were dried at  $120^\circ\text{C}$  in vacuum and pressed. Metallic sodium was used as an anode electrode. The electrolyte solution used was  $1.0 \text{ mol l}^{-1}$   $\text{NaPF}_6$  dissolved in propylene carbonate (PC). The loading in the electrode was about  $5 \text{ mg cm}^{-2}$ . A glass fiber was used as a separator. R2032-type coin cells were assembled in the Ar-filled glove box. Cyclic voltammetry (CV), (Model VMP3; NanoQuébec), was performed with  $10 \mu\text{V s}^{-1}$  scan rate. For galvanostatic experiments, the cells were discharged-charged galvanostatically at a constant current. To identify the kinetics of the bare and DN-coated NFMO, the activated two-electrode cells (working: NFMO, counter and reference: Na) were subjected to electrochemical impedance spectroscopy (EIS) before cell cycling, with a sinusoidal voltage signal (5 mV) over a frequency ranging from 100 kHz to 100 mHz.

## Results and discussion

Fig. 1(a) shows a scheme of the carbon-coating. First, a mixture of NFMO and DN was heat-treated at  $300^\circ\text{C}$  for 1 h under  $\text{N}_2$  flow to allow DN through a dehydration reaction. In this step, DN is chemisorbed onto the surface of the cathode material. Then, the DN-coated NFMO was heat-treated at  $550^\circ\text{C}$  for 3 h under  $\text{N}_2$  flow to carbonize DN. Most DN molecules are carbonized without desorption and a thin carbon layer remains, which uniformly covers the NFMO surface.<sup>17</sup>

To confirm the effects of the carbon coating on the cathode structure, XRD measurements were performed. Fig. 1(b) shows XRD patterns of the pristine, 0.1, 0.2, and 0.5 wt%-DN-coated

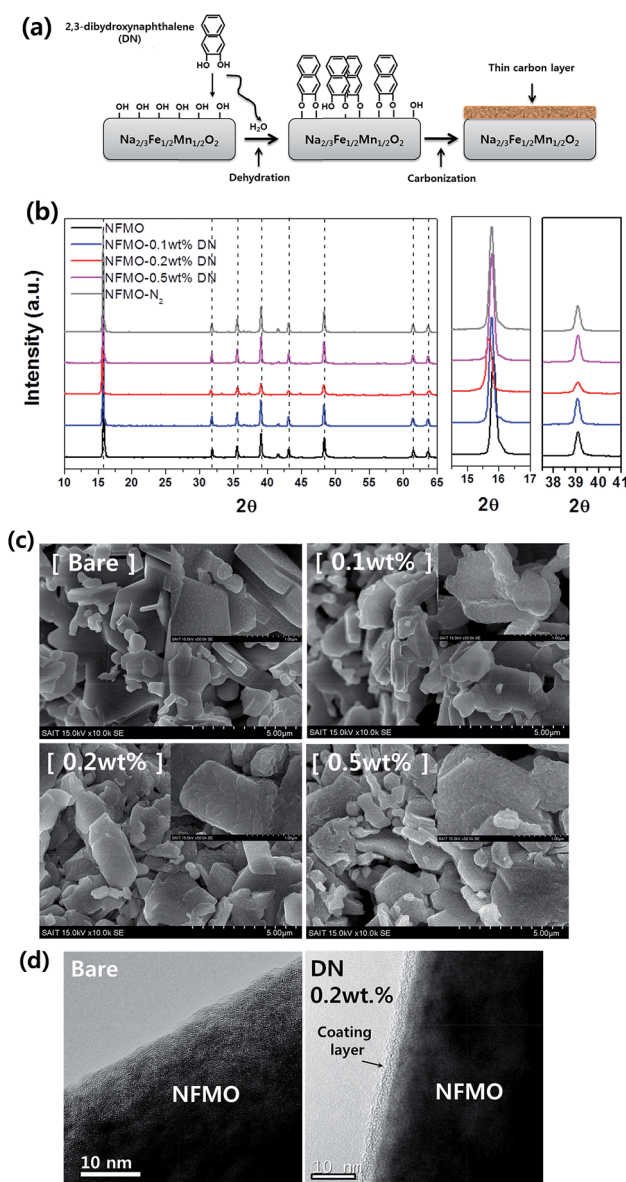


Fig. 1 (a) A scheme of the uniform carbon-coating process (b) XRD patterns of DN coated NFMO powders (c) SEM images of DN coated NFMO powders (d) TEM images of bare NFMO and 0.2 wt% DN coated NFMO.

samples. All samples show well-defined characteristics matching that of a P2-type layered structure seen in previous studies.<sup>1,6</sup> A small increase in the lattice parameter of the coated samples is discussed in ESI 1.† This increase might be due to an increase in repulsion between oxygen layers caused by the decrease in Na (ESI 2†) during the coating process. Moreover, no impurity peaks appear in the XRD patterns of coated samples. This indicates that the thin DN coating layer did not change the host structure of the active material. SEM images of the pristine, 0.1, 0.2, and 0.5 wt%-DN-coated samples are shown in Fig. 1(c). All samples showed flake shaped crystals with similar particle size. Morphology of the three coated powders indicated little change during the coating process in a reducing environment. For coated samples, the coating layer is hardly noticeable; the carbon layer on the material is expected to be very thin and uniform.

TEM images of pristine and 0.2 wt%-DN-coated sample are shown in Fig. 1(d); these two images confirm a very thin (about 5 nm) and uniform carbon layer on the coated cathode surface in contrast to the clear surface of the bare material. The electrical conductivities of pristine, 0.1, 0.2, and 0.5 wt%-DN-coated NFMOs, as measured by the four-point probe method, were  $1.216 \times 10^{-6} \text{ S cm}^{-1}$ ,  $1.92 \times 10^{-6} \text{ S cm}^{-1}$ ,  $2.10 \times 10^{-6} \text{ S cm}^{-1}$ , and  $3.104 \times 10^{-6} \text{ S cm}^{-1}$ , respectively. Even though the differences are small, the higher conductivity of NFMO/C powder is attributed to a carbon layer on the powder surface. Thermal gravimetric analysis (TGA) was performed to provide corroboration of the existence of a carbon layer. Thermal decomposition of powder samples was analyzed from room temperature to 800 °C in flowing air; the weight changes of powders are listed in Table 1. The weight losses of powders corresponded to increased coating contents. In the 0.5 wt% DN-coated sample, a sharp exothermal peak was not observed, because the weight percentage of the coating layer was very less. However, a small peak appeared between 300 °C and 400 °C in the differential scanning calorimetry (DSC) data (ESI 3†).

Fig. 2(a) compares the cycling performance of the cells at 25 °C with a constant rate of 0.1 C. The capacity retentions are 77.8%, 59.3%, 77.7%, and 62.4% at the 50th cycle for bare NFMO and 0.1, 0.2, and 0.5 wt%-DN-coated samples, respectively. The capacity fading of DN-coated samples and NFMO heated in a reducing atmosphere (capacity 59.9% at 50th cycle) is higher than that of bare NFMO. This may correspond to an unstable structure caused by Fe reduction.

Blesa *et al.* reported that only 0.1 mol of sodium of NaFeO<sub>2</sub> had to participate in electrochemical reaction for a reversible reaction.<sup>20</sup> Alternatively, the fast capacity fading occurred because of an increase in activation energy caused by degradation of crystallinity. The NFMO formulation was based on NaFeO<sub>2</sub>, using Mn substitution for increasing capacity.<sup>1</sup>

Table 1 The DSC results of samples

Sample name	Bare	0.1 wt%	0.2 wt%	0.5 wt%
Weight loss (%)	2.51	2.65	2.92	3.95

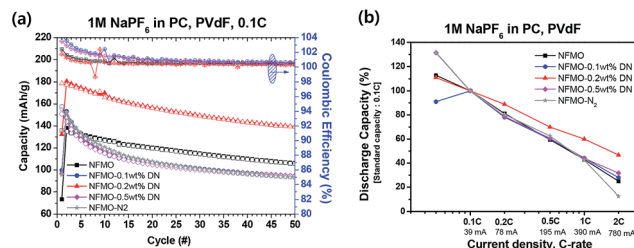


Fig. 2 (a) Cycling performance comparison of bare NFMO and DN coated NFMOs (b) relative comparison of rate capabilities of bare NFMO and DN coated NFMOs.

Therefore, the increased participation of Fe in electrochemical reactions as a result of the heat treatment in a reducing atmosphere increases the capacity degradation. The 0.2 wt%-DN-coated NFMO showed the lowest capacity fading because of this effect. On the other hand, the high capacity fading for 0.5 wt% DN was due to the decline of sodium mobility. However, 0.2 wt%-DN-coated NFMO sustained very similar retention compared to bare NFMO, because of the prevention of direct contact between cathode and electrolyte, as well as improvement of reaction kinetics during establishment of the desired uniform thickness of carbon layer.

Rate capabilities for all samples were evaluated next by cycling at various rates from 0.05 to 2 C, and the results are presented in Fig. 2(b). As the applied current was increased, the capacities of all samples decreased. This observation can be ascribed to an increase in over-potential resulting from the lack of reaction time for mobile cation intercalation into the crystal lattice; in consequence, only the surface of the active materials participates in the reaction.<sup>4</sup> At high applied current density (more than 0.2 C), the values of capacity for all samples excluding 0.2 wt%-DN-coated NFMO are almost same. However, 0.2 wt%-DN-coated NFMO showed the higher capacity at all applied current densities, resulting from the enhancement in electronic conductivity and facile migration of Li-ions through the thin and uniform carbon layers that were coated on the surface on NFMO active particles. After the C-rate tests, the original capacities of both samples were restored (ESI 4†).

The electrochemical reactions of samples were confirmed by CV analysis, and the results are shown in Fig. 3(a). All samples show similar peak positions of anode and cathode. The anodic peaks at around 2.4 V and 3.9 V and cathodic peaks at around 2.0 V and 3.2 V correspond to the intercalation and extraction processes of mobile Na<sup>+</sup> ions; these values are similar to those in a previous study.<sup>1,6</sup> The sharp increase in the anodic curve at around 4.2 V is related to a quasi-reversible P2-type-to-O2-type phase transition occurring at low Na content in the material.<sup>1,5,6</sup> The lower cathodic peak is related to the Mn redox process, while the higher cathodic peak is from Fe redox. The higher cathodic peaks of active materials, which were heat-treated under N<sub>2</sub> flow, including DN-coated samples, are enlarged. This indicates an increase in the number of reaction sites for Fe redox reaction. The number of reaction sites for Mn also increased but does not show a remarkable difference, unlike in the number of reaction sites for Fe.



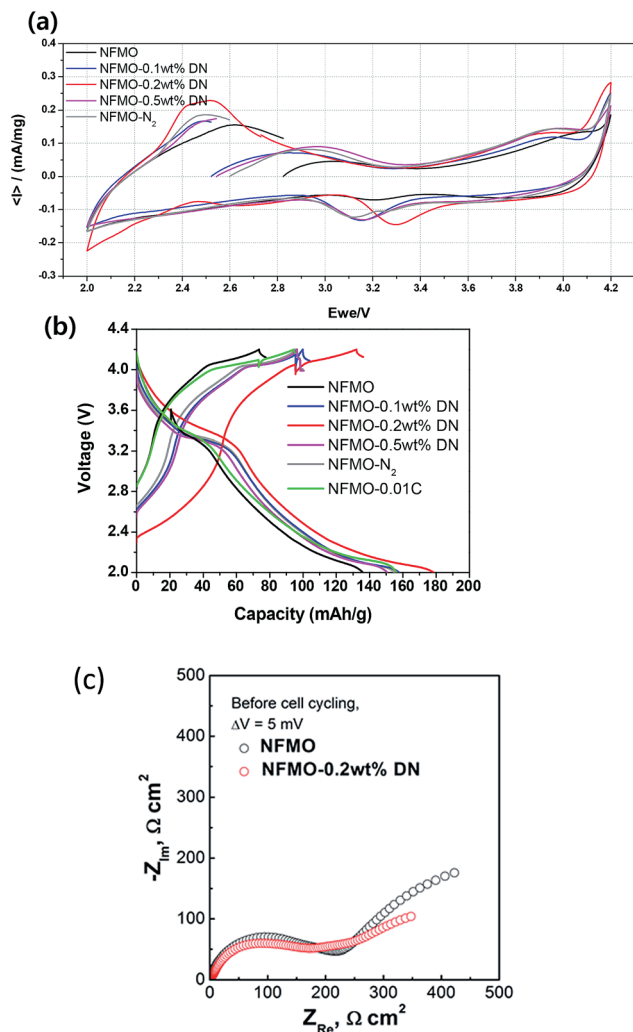


Fig. 3 (a) Comparison of cyclic voltammograms (b) comparison of typical charge–discharge characteristics. (c) EIS spectra of bare and 0.2 wt% DN coated NFMO measured before cell cycling.

Fig. 3(b) shows the potential *versus* capacity profiles of NFMO and NFMO/C during the 1st cycle at 0.1 C, with profiles for both materials showing a similar slope, as well as other features. The location of the potential plateau was consistent with the results of CV experiments; the profile for active materials processed in a reducing atmosphere exhibited a wider plateau than those for bare NFMO did, indicating the existence of more reaction sites. At a cutoff voltage of 2.0 V, the cells delivered reversible capacities of  $\sim 135.9 \text{ mA h g}^{-1}$ ,  $\sim 157.6 \text{ mA h g}^{-1}$ ,  $\sim 178.7 \text{ mA h g}^{-1}$ , and  $\sim 150.8 \text{ mA h g}^{-1}$  for bare NFMO and 0.1, 0.2, and 0.5 wt%-DN-coated samples, respectively. Although NFMO heated in a reducing atmosphere showed a similar capacity of  $\sim 155.0 \text{ mA h g}^{-1}$ , the length of the plateau and the capacity increased. This might be due to the elimination of remaining impurities on the surface and the increase in the number of reaction sites due to the reducing heat treatment. Surface impurities may lead to performance deterioration as a result of interference with Na-ion transfer. When bare NFMO is tested with very low discharge–charge current (1/100 C), a capacity ( $\sim 156.1 \text{ mA h g}^{-1}$ ) similar to that of

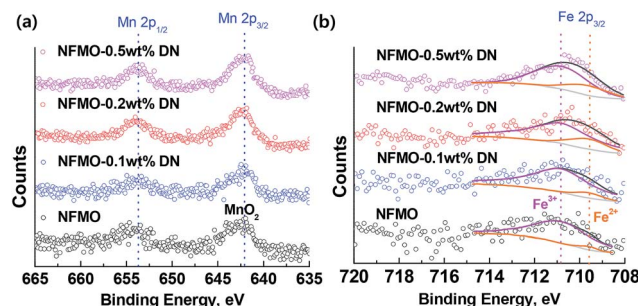


Fig. 4 XPS core peaks of bare NFMO and DN coated NFMOs (a) Mn 2p (b) Fe 2p.

Table 2  $\text{Fe}^{2+}/\text{Fe}^{3+}$  ratios in the pristine and DN-coated NFMO estimated from the deconvolution of their Fe 2p<sub>3/2</sub> XPS core peaks

Sample name	Bare	0.1 wt%	0.2 wt%	0.5 wt%
$\text{Fe}^{2+}/\text{Fe}^{3+}$ ratio	0.036	0.068	0.203	0.323

NFMO heated in a reducing atmosphere was measured, as shown in Fig. 3(b). Similar results have been reported by other groups.<sup>18,19</sup> Along with this effect, the improvement in the conductivity for 0.1 wt% and 0.2 wt%-DN-coated NFMO also resulted in a higher capacity compared to bare NFMO. However, the capacity of 0.5 wt%-DN-coated NFMO was less due to a decrease in the  $\text{Na}^+$  ion mobility from the thicker coating layer. The 0.2 wt%-DN-coated sample showed the highest capacity because of the enhancement of kinetic effects such as increase of Fe redox and high electric conductivity. We also found from the EIS spectra of the bare and 0.2 wt%-DN-coated NFMO that the charge transfer resistance on the surfaces of DN (0.2 wt%) coated NFMO particles was much lower compared with bare NFMO, indicative of superior kinetics of the DN coated NFMO to the uncoated NFMO, shown in Fig. 3(c).

For a more direct confirmation, XPS analysis was carried out; the results are shown in Fig. 4. The Mn 2p XPS spectra for the active materials showed that the oxidation state of Mn in pristine NFMO was +4 and it remained unchanged by DN coating. Variation in the oxidation states of Fe in the samples was observed by deconvoluting their Fe 2p<sub>3/2</sub> XPS core peaks. The Fe oxidation state in NFMO decreased with an increase in the amount of DN (Table 2), indicating that Fe ions but not Mn located near the surface of NFMO particles tend to be reduced by the oxidation of DN during annealing. Using the DN coating process, thin and uniform carbon coating layer was formed on cathode material and the electrochemical performance was enhanced by that carbon layer.

## Conclusions

To obtain a thin, uniform carbon coating on  $\text{Na}_{2/3}\text{Fe}_{1/2}\text{Mn}_{1/2}\text{O}_2$  (NFMO), 2,3-dihydroxynaphthalene (DN) was used. An amorphous carbon nanolayer was obtained on the surface of layered pristine material. During the coating process, the number of

active Fe sites increased as a result of heat treatment in a reducing atmosphere and the conductivity was enhanced by the carbon layer. Among various coating content levels, 0.2 wt% DN-coated NFMO exhibits the best electrochemical performance. An initial discharge capacity of  $178 \text{ mA h g}^{-1}$  is obtained at a C-rate of 0.1 C. This capacity is 20% larger than that of bare NFMO. Capacity retention (82% at the 30th cycle) also remains higher in comparison to bare NFMO.

## Notes and references

- 1 N. Yabuuchi, M. Kajiyama, J. Iwatate, H. Nishikawa, S. Hitomi, R. Okuyama, R. Usui, Y. Yamada and S. Komaba, *Nat. Mater.*, 2012, **11**, 51.
- 2 V. Palomares, P. Serras, I. Villaluenga, K. Hueso, J. Carretero-González and R. Teófilo, *Energy Environ. Sci.*, 2012, **5**, 5884.
- 3 S. Komba, C. Takei, T. Nakayama, A. Ogata and N. Yabuuchi, *Electrochem. Commun.*, 2010, **12**, 355.
- 4 E. Hosono, T. Saito, J. Hoshino, M. Okubo, Y. Saito, D. Nishio-Hamane, T. Kudo and H. Zhou, *J. Power Sources*, 2012, **217**, 43.
- 5 R. Berthelot, D. Carlier and C. Delmas, *Nat. Mater.*, 2011, **10**, 74.
- 6 K. Park, D. Han, H. Kim, W. Chang, B. Choi, B. Anass and S. Lee, *RSC Adv.*, 2014, **43**, 22798.
- 7 T. Zhao, S. Chen, L. Li, X. Zhang, R. Chen, I. Belharouak, F. Wu and K. Amine, *J. Power Sources*, 2013, **228**, 206.
- 8 S. Lee, S. Oh, W. Cho and H. Jang, *Electrochim. Acta*, 2006, **52**, 1507.
- 9 B. Huang, X. Li, Z. Wang, H. Guo, X. Xiong and J. Wang, *J. Alloys Compd.*, 2014, **583**, 313.
- 10 Y. Kim, H. Kim and S. Martin, *Electrochim. Acta*, 2006, **52**, 1316.
- 11 S. Shi, J. Tu, Y. Mai, Y. Zhang, C. Gu and X. Wang, *Electrochim. Acta*, 2012, **63**, 112.
- 12 H. Takahara, T. Takeuchi, M. Tabuchi, H. Kageyama, Y. Kobayashi, Y. Kurisu, S. Kondo and R. Kanno, *J. Electrochem. Soc.*, 2004, **151**, A1539.
- 13 H. Kim, M. Kong, K. Kim, I. Kim and H. Gu, *J. Power Sources*, 2007, **171**, 917.
- 14 J. Ni, L. Gao and L. Lu, *J. Power Sources*, 2013, **221**, 35.
- 15 Y. Lu, S. Zhang, Y. Li, L. Xue, G. Xu and X. Zhang, *J. Power Sources*, 2014, **247**, 770.
- 16 Z. Jian, L. Zhao, H. Pan, Y. Hu, H. Li, W. Chen and L. Chen, *Electrochem. Commun.*, 2012, **14**, 86.
- 17 T. Kwon, H. Nishihara, Y. Fukura, K. Inde, N. Setoyama, Y. Fukushima and T. Kyotani, *Mesoporous Mater.*, 2010, **132**, 421.
- 18 H. Nishihara, Y. Fukura, K. Inde, K. Tsuji, M. Takeuchi and T. Kyotani, *Carbon*, 2008, **46**, 48.
- 19 H. Nishihara, Y. Fukura, K. Inde, K. Tsuji, M. Takeuchi and T. Kyotani, *Carbon*, 2008, **46**, 48.
- 20 M. Blesa, E. Moran, C. León, J. Santamaria, J. Tornero and N. Menéndez, *Solid State Ionics*, 1999, **126**, 81.